STEM CELLS TRANSLATIONAL MEDICINE®

PLURIPOTENT STEM CELLS

Impact of Feeding Strategies on the Scalable Expansion of Human Pluripotent Stem Cells in Single-Use Stirred Tank Bioreactors

CHRISTINA KROPP,[a,b] HENNING KEMPF,[a,b] CAROLINE HALLOIN,[a,b] DIANA ROBLES-DIAZ,[a,b] ANNIKA FRANKE,[a,b] THOMAS SCHEPER,[c] KATHARINA KINAST,[d] THOMAS KNORPP,[e] THOMAS O. JOOS,[e] AXEL HAVERICH,[a,b] ULRICH MARTIN,[a,b] ROBERT ZWEIGERDT,[a,b,*] RUTH OLMER[a,b,*]

Key Words. Human pluripotent stem cell expansion • Induced pluripotent stem cells • Perfusion • Three-dimensional suspension culture • Single-use stirred tank bioreactors • Metabolism

[a]Department of Cardiac, Thoracic, Transplantation, and Vascular Surgery, Leibniz Research Laboratories for Biotechnology and Artificial Organs, Hannover, Germany; [b]REBIRTH–Cluster of Excellence, Hannover Medical School, Hannover, Germany; [c]Institute of Technical Chemistry, Gottfried-Wilhelm-Leibniz University Hannover, Hannover, Germany; [d]Eppendorf AG Bioprocess Center, Juelich, Germany; [e]Natural and Medical Science Institute (NMI) at the University of Tuebingen, Reutlingen, Germany

[*]Contributed equally.

Correspondence: Robert Zweigerdt, Ph.D., Leibniz Research Laboratories for Biotechnology and Artificial Organs, Hannover Medical School, Carl-Neuberg-Strasse 1, 30625 Hannover, Germany. Telephone: 49 511 532 5023; E-Mail: zweigerdt.robert@mh-hannover.de

Received September 16, 2015; accepted for publication April 20, 2016; published Online First on July 1, 2016.

1066-5099/2016/$20.00/0

http://dx.doi.org/10.5966/sctm.2015-0253

ABSTRACT

The routine application of human pluripotent stem cells (hPSCs) and their derivatives in biomedicine and drug discovery will require the constant supply of high-quality cells by defined processes. Culturing hPSCs as cell-only aggregates in (three-dimensional [3D]) suspension has the potential to overcome numerous limitations of conventional surface-adherent (two-dimensional [2D]) cultivation. Utilizing single-use instrumented stirred-tank bioreactors, we showed that perfusion resulted in a more homogeneous culture environment and enabled superior cell densities of 2.85 × 10^6 cells per milliliter and 47% higher cell yields compared with conventional repeated batch cultures. Flow cytometry, quantitative reverse-transcriptase polymerase chain reaction, and global gene expression analysis revealed a high similarity across 3D suspension and 2D precultures, underscoring that matrix-free hPSC culture efficiently supports maintenance of pluripotency. Interestingly, physiological data and gene expression assessment indicated distinct changes of the cells' energy metabolism, suggesting a culture-induced switch from glycolysis to oxidative phosphorylation in the absence of hPSC differentiation. Our data highlight the plasticity of hPSCs' energy metabolism and provide clear physiological and molecular targets for process monitoring and further development. This study paves the way toward more efficient GMP-compliant cell production and underscores the enormous process development potential of hPSCs in suspension culture. STEM CELLS TRANSLATIONAL MEDICINE *2016;5:1289–1301*

SIGNIFICANCE

Human pluripotent stem cells (hPSCs) are a unique source for the, in principle, unlimited production of functional human cell types in vitro, which are of high value for therapeutic and industrial applications. This study applied single-use, clinically compliant bioreactor technology to develop advanced, matrix-free, and more efficient culture conditions for the mass production of hPSCs in scalable suspension culture. Using extensive analytical tools to compare established conditions with this novel culture strategy, unexpected physiological features of hPSCs were discovered. These data allow a more rational process development, providing significant progress in the field of translational stem cell research and medicine.

INTRODUCTION

The scope for the application of human pluripotent stem cell (hPSC)-derived progenies ranges from regenerative medicine to in vitro disease modeling, safety pharmacology, and innovative drug discovery [1]. A prerequisite for all applications is the supply of cells in meaningful quantities and constant quality [2, 3]. Standard cultivation methods for the expansion of hPSCs at the pluripotent state conventionally rely on adherence to culture substrates (two-dimensional [2D])—either on feeder cells or on cell-free matrices—and often deploy passaging of semidissociated cell clumps, hampering process inoculation by exact cell numbers [4]. Moreover, 2D culture in typical dishes and flasks allows very restricted monitoring of culture parameters, thereby limiting systematic process control and optimization [3].

In industry, using common mammalian cell lines such as 293T or CHO cells for the production of vaccines or recombinant proteins, respectively, parallel stirred-tank bioreactor systems are widely used for multifactorial process development in relatively small suspension culture (three-dimensional [3D]) scale [5]. These systems support linear process

upscaling employing equivalent bioreactor design in larger dimensions. Stirred-tank bioreactors ensure homogeneous distribution of cells, nutrients, and gases; allow tight monitoring and control of key process parameters such as pH and dissolved oxygen (DO); and support flexible, automated feeding strategies [3].

Recently, we and others established single-cell inoculated hPSCs expansion as cell-only aggregates in static and dynamic suspension culture [6–11]. The approach overcomes the need for matrices required in feeder-free 2D cultures or microcarrier-based suspension culture [12, 13], thereby reducing the number of culture components and supporting GMP compliance. Transfer to stirred-tank bioreactors with final cell densities of $\sim 2 \times 10^6$ cells per milliliter was readily achieved via the aggregate method [9, 14, 15], yielding $\sim 2 \times 10^8$ pluripotent hPSCs in a 100-ml scale bioreactor run [15]. But estimated cell requirements for heart and liver repair as well as diabetes treatment amount to 10^9–10^{10} hPSC-derived progenies per patient [3]. This implies that significant process improvement is required in addition to further scale-up.

Previous studies on hPSC suspension culture mainly focused on repeated batch processes, i.e., exchanging the entire culture medium in 24-hour intervals [7–9, 11, 15, 16]. However, despite the modulation of inoculation parameters and stirring conditions, growth kinetics revealed linear rather than the desired exponential cell expansion.

Advanced stirred-tank bioreactors can be equipped with cell retention systems enabling perfusion [17–19]. This feeding strategy is characterized by continuous medium replacement [17], avoiding the drastic daily "nick" provoked in repeated batch cultures. Work on mouse embryonic stem cells (ESCs) showed that perfusion can indeed improve process efficiency [20, 21] but very limited studies on human PSCs are yet available [12, 22].

Taking advantage of fully instrumented single-use bioreactors, the aim of this study was to develop hPSC expansion in suspension toward GMP compliance. By closely comparing alternative feeding strategies, we shed light on physiological, cellular, and molecular changes in response to process modification. In addition, we have identified a switch in hPSCs' energy metabolism from glycolysis to oxidative phosphorylation in response to the culture environment in the absence of hPSC differentiation, which is a key finding regarding rational process development.

Materials and Methods

Bioreactor System

The present study was performed using a DASbox Mini Bioreactor System (Eppendorf AG, Hamburg, Germany, https://www.eppendorf.com) for parallel operation of four or more independently controllable BioBLU 0.3 Single-Use Vessels (supplemental online Fig. 1A) equipped with an eight-blade impeller (60° pitch) optimized for hPSC expansion [15]. A magnet-coupled overhead drive allowed smooth agitation. Sensors for pH and DO monitoring as well as temperature control ensured a tight monitoring and control of critical process parameters. Pumps and sensor were calibrated as described previously [23].

Perfusion was technically established by the incorporation of a porous filter (20- to 40-μm pore size) as a cell retention device similar to that in Weegman et al. [24]. The culture volume was kept constant by applying the same flow rates for addition of fresh medium (feed) via a head plate port and for the removal of depleted medium (waste) via the outflow filter (supplemental online Fig. 1B).

Cell Culture

Experiments were performed utilizing the human induced pluripotent stem cell (hiPSC) lines hCBiPS2 [25] and hHSC_F1285T_iPS2 [26] from cord blood-derived endothelial cells or hematopoietic stem cells, respectively. Ahead of process inoculation hiPSCs were expanded in feeder-free monolayer culture on Geltrex-coated (Invitrogen; ThermoFisher, Waltham, MA, http://www.thermofisher.com) flasks either in E8 for hHSC_F1285T_iPS2 cells or in mTeSR1 (STEMCELL Technologies, Vancouver, BC, Canada, http://www.stemcell.com) or in KnockOUT-SR medium (Life Technologies, ThermoFisher) conditioned with murine embryonic fibroblasts (MEFs) for hCBiPS2 cells for at least four passages as described in detail elsewhere [23]; monolayer cultures were started from conventional MEF-based cultures as described elsewhere [23]. Precultures for bioreactor inoculation did not exceed eight passages in feeder-free monolayer culture.

Bioreactor Inoculation and Process Parameters

Bioreactors were inoculated with a single-cell suspension to achieve a viable cell density of 5×10^5 cells per milliliter in mTeSR1 for hCBiPS2 or E8 for hHSC_F1285T_iPS2 cells + 10 μM Y-27632 (synthesized as previously described [27]) in a final 125-ml culture volume (62.5 million cells per vessel) as previously described [23]. Cells were cultivated at 37°C, stirred at 60–70 revolutions per minute (rpm), and aerated with 3 sl/hour of 21% O_2 and 5% CO_2. No media changes were performed for 2 days after single-cell inoculation. Afterward, for repeated batch processes 100 ml of culture medium was manually replaced once every 24-hour interval, thereby excluding cell loss. For perfusion, the culture medium was constantly replaced at flow rates of 4.2 ml/hour, which is equivalent to $\approx$100 ml/day, while cell aggregates are retained inside the bioreactor by the cell retention device.

Sampling, Aggregate Analysis, and Cell Counting

Sampling from the bioreactors was performed without interruption of stirring as described earlier [23]. To prevent culture dilution, the sample volume was not replaced, resulting in culture volume reduction from 125 ml to approximately 100 ml in the 7-day lasting processes.

To monitor aggregate formation and diameters (d), up to 10 independent light microscopic images were captured for each sample (Axiovert A1; Zeiss, Thornwood, NY, http://www.zeiss.com) followed by diameter analysis via Axiovision 8.4 software. Mean diameters represent arithmetic averages of 240–1,480 single aggregates. For an example of used images see supplemental online Figure 1C. Aggregate volume was calculated as $V = (4/3)\pi r^3$ with $r = (1/2)d$.

For cell counting and flow cytometry, aggregates were dissociated into single cells with collagenase B as described earlier [8, 23]. Supernatant was stored at – 20°C for subsequent analyses (supplemental online data).

Statistical Analysis

All bioreactor runs were performed in three or four independent runs. Thereby, for every independent run, repeated-batch and perfusion bioreactors were inoculated in parallel, applying cells from the same 2D preculture-derived suspension. Statistical analyses were performed with GraphPad Prism6 after performing block correction using the preculture as blocking factor. Statistical

significance was determined by ordinary one-way ANOVA or two-way ANOVA followed by Bonferroni's post-test. Thereby differences were considered statistically significant at $p < .05$, $p < .01$, and $p < .001$. Results are reported as mean and standard error of mean (SEM).

RESULTS

Differential hPSC Aggregate Size Is Induced by Alternative Feeding Strategies

Cultures were inoculated with single-cell suspensions (schematic in Fig. 1A) at 5×10^5 cells per milliliter in single-use vessels (supplemental online Fig. 1A) and randomly attributed to repeated batch or perfusion on day 2. The medium throughput was set to 100 ml/day at both conditions, adding up to 500 ml/process (feeding circuit schematic in supplemental online Fig. 1B). Assessing aggregate formation (Fig. 1B, 1C; supplemental online Fig. 1C) revealed 58.3 ± 4.1 μm average diameter on day 2. Significant feeding-dependent differences became apparent from day 5 onward, resulting in an average diameter of 123.0 ± 10.1 μm (repeated batch) versus 133.9 ± 9.8 μm (perfusion) on day 7 (Fig. 1C). Volume calculation pronounced process-dependent aggregate divergence that was increased by 33% in perfusion on day 7 (Fig. 1D). Notably, no inadvertent cell loss, e.g., due to the attachment of cells or aggregates to vessel or sensors, was observed throughout the study.

Perfusion Results in 47% Higher Cell Yields

The expected drop of viable cell counts and viability at 24 hours postinoculation (day 1, Fig. 2A) is in line with our previous study [15] and was readily overcompensated at 48 hours, reflected by the recovery of viability and the highest specific growth rate (μ) of 0.81 ± 0.18 day^{-1} on day 2 (Fig. 2B). Repeated batch resulted in an average cell density of $1.94 \pm 0.16 \times 10^6$ cells per milliliter on day 7, representing an approximately fourfold increase of inoculated cell numbers. Perfused cultures reached a maximal density of up to 3.6×10^6 cells per milliliter in individual runs (not shown) and $2.85 \pm 0.34 \times 10^6$ cells per milliliter on average (Fig. 2A), representing a significant increase of 47% over repeated batch and an approximately sixfold expansion rate in the 7-day lasting bioreactor processes. Constant viability was observed on process days 3–7 in perfusion whereas a slight drop was noted on days 6 and 7 in repeated batch cultures (Fig. 2A).

Repeated batch induced "zig-zag patterns" of glucose and lactate levels in contrast to continuous progression at perfusion (Fig. 3A, 3B). No more than 60% of the available glucose was consumed at any time and peak levels of lactate did not exceed 14 mM. The corresponding yield coefficient of lactate from glucose (Y(qLac/qGlc)) was ~2 on day 2, thus integrating between values of 1.8 and 2.8 reported for hESCs in other platforms [14, 28, 29]. Y(qLac/qGlc) remained higher at perfusion on days 3 and 4. However, from day 5 onward, Y(qLac/qGlc) decreases to ~1.6 for both feeding strategies (Fig. 3C). For 2D precultures Y(qLac/qGlc) values integrate between 1.9 and 2.1 until day 3, that is, before cells were used for bioreactor inoculation.

The daily medium exchange in repeated batch cultures resulted in a sharp, transient restoration of pH and DO as well as osmolarity levels whereas those parameters continuously progressed in perfused cultures (Fig. 3D–3F). Lowest pH values of ~6.6 were notably similar for both culture conditions (Fig. 3D).

Minor process-dependent differences in amino acids consumption were detected (supplemental online Fig. 2) and none were depleted including glutamine, known to be a major energy source and limiting factor in mammalian cell culture [30]. However, glutamate, alanine, and to some extent glycine were found to be accumulated, which was, by trend, more prominent at repeated batch conditions (supplemental online Fig. 2).

Slight Accumulation of Chemokine C-X-C Motif Ligand 5 in Supernatant From Perfusion

Multi-analyte profiling (MAP) of day 7 culture supernatants revealed a significant accumulation of the chemokine C-X-C motif ligand 5 (CXCL5) at perfusion, but no differences for basic fibroblast growth factor (bFGF) levels were detected between both feeding strategies. However, compared with fresh culture medium, an ~80% drop in bFGF concentration in 24 hours (from process day 6 to day 7) was noted (supplemental online Fig. 3A). Investigating recombinant CXCL1 and -5 supplementation revealed a slight concentration-dependent proliferation support of CXCL5 in a static suspension culture assay (supplemental online Fig. 3B). In contrast, no effect of CXCL1 at concentrations previously shown to enhance human ESC proliferation in monolayer was observed [31].

hPSCs' Pluripotency and Differentiation Potential Is Maintained at Both Feeding Conditions

Immunofluorescence staining (Fig. 4A) and flow cytometry (Fig. 4B) of day 7 samples revealed that, regardless of feeding conditions, the majority of cells (i.e., 90.0%–97.9%, respectively) were positive for octamer binding transcription factor 4 (*OCT4*), *NANOG*, stage-specific embryonic antigen4 (*SSEA4*), and stage-specific embryonic antigen3 (*SSEA3*) equivalent to 2D precultures. Ki-67 staining on sections underlined the proliferative state of cells within aggregates harvested at process endpoint (Fig. 4A).

Undirected differentiation of day 7 aggregates resulted in cell types representative of all three germ layers as evidenced by immunofluorescence staining (Fig. 5A). Furthermore, directed differentiation via chemical Wnt pathway modulators [23, 32] supported cardiomyogenic differentiation as shown by flow cytometry specific to sarcomeric actinin (SA) and myosin heavy chain (MHC), with similar efficiencies for repeated batch- and perfusion-derived aggregates (Fig. 5B).

Global Transcriptome Analysis Reveals Vast Similarities but Vocal Platform- and Feeding-Dependent Differences

Quantitative reverse-transcriptase polymerase chain reaction (qRT-PCR) of 3D bioreactor samples on day 7 versus 2D precultures revealed equivalent expression of pluripotency-associated transcription factors OCT4 and NANOG (Fig. 6A). This was confirmed for numerous pluripotency and early differentiation-associated markers by global gene expression arrays (Fig. 6B). Only for *T* a significant but negligible difference was found between the different process conditions.

The schematic in supplemental online Figure 4A displays the entire range of samples compared by expression arrays: 2D precultures at day 3, static suspension culture at day 3, and stirred (i.e., bioreactor-derived) repeated batch or perfusion suspension culture at day 3 and day 7.

Principle component analysis (PCA) revealed close proximity of day 3 static and stirred suspension irrespective of the feeding strategy, suggesting minor impact only of stirring stress on gene

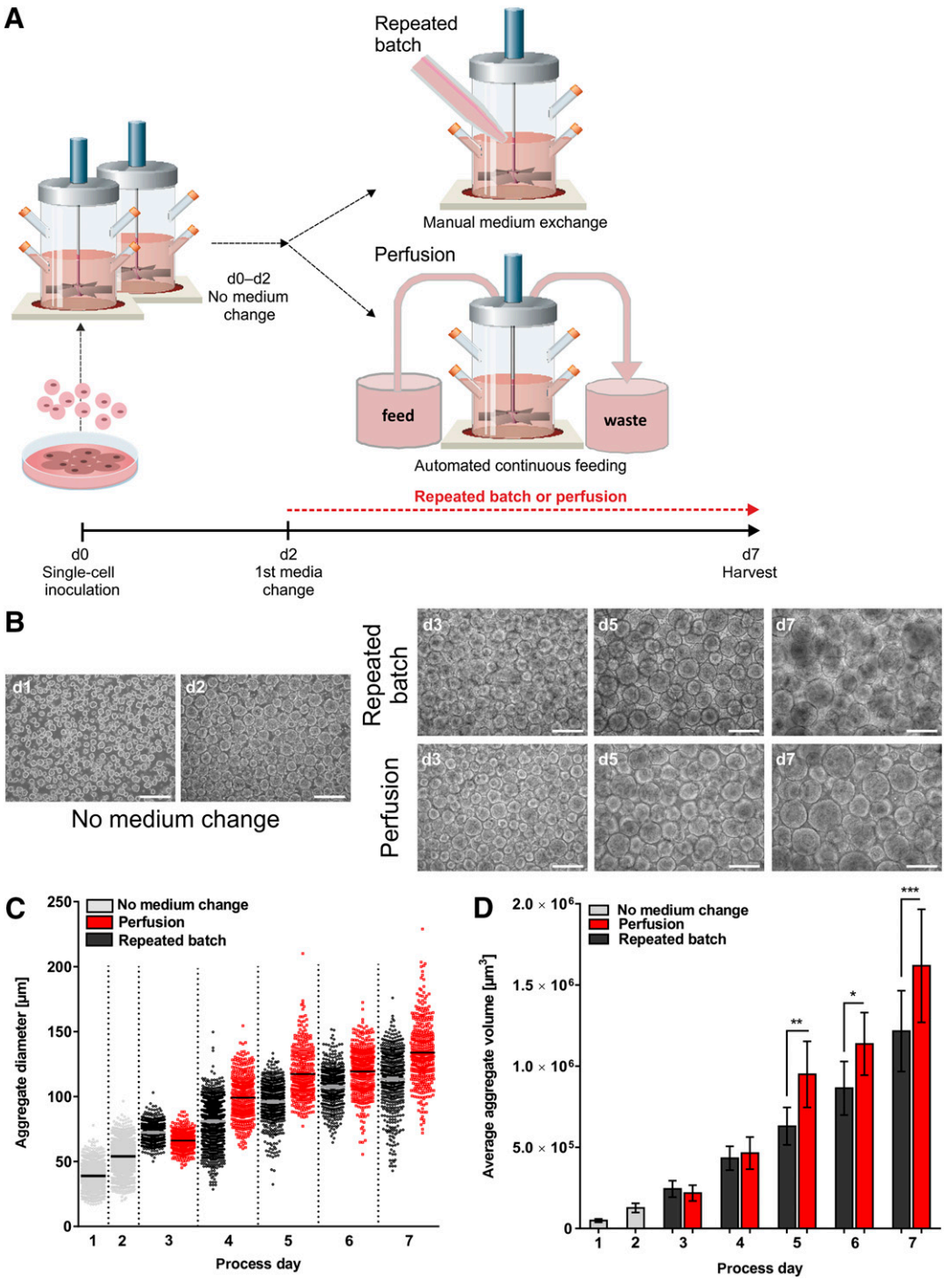

Figure 1. Impact of feeding strategies on aggregate formation and size distribution. **(A):** Human induced pluripotent stem cells (hCBiPS2) were detached from monolayer cultures and seeded as single-cell suspensions on day 0 to stirred tank bioreactors. During the first 48 h cultures were maintained without any medium exchange. On culture day 2 the first complete manual medium exchange was performed for the repeated batch cultures (repeated the following days [days 3–6]), and in parallel automated continuous medium change was started for the perfusion cultures (4.2 ml/hour), resulting in equal medium throughput for both feeding strategies. On culture day 7 cells from both processes were harvested and analyzed. **(B):** On process days 1 and 2 (prior to perfusion start and first manual medium change in repeated batch bioreactors) as well as days 3–7 aggregates were assessed by light microscopy as shown (scale bars = 200 μm). **(C):** Applying AxioVision LE (Zeiss) and GraphPad prism software, between 240 and 1,480 aggregates from four independent experiments were analyzed (supplemental online Fig. 1C) from each time point and visualized as single squares. **(D):** The average aggregate volume calculated from the mean aggregate volume of the individual runs is depicted as columns whereby each column represents the mean of four independent bioreactor runs for each feeding strategy. Results are reported as mean ± SEM. Differences were considered statistically significant at *, $p < .05$, **, $p < .01$, and ***, $p < .001$. Abbreviation: d, day.

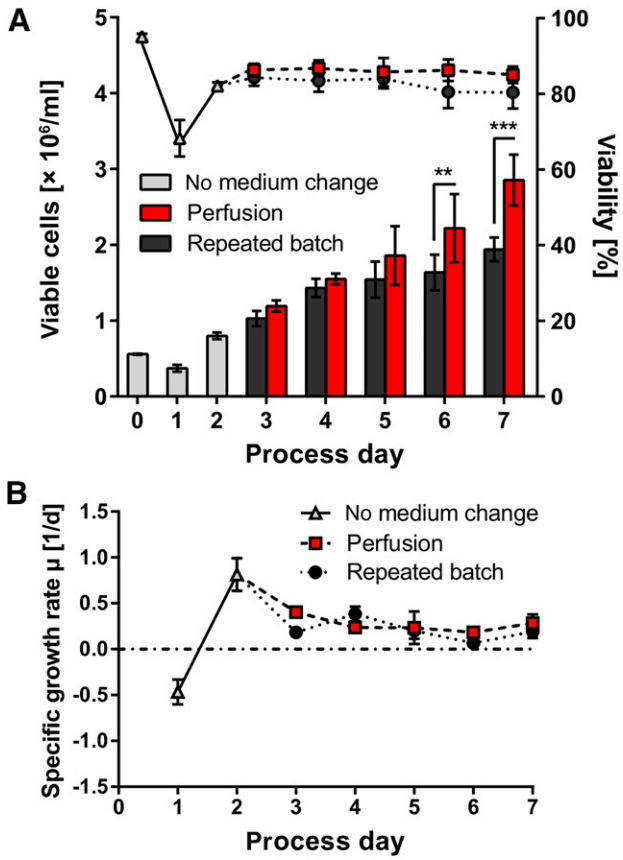

Figure 2. Comparison of growth kinetics and viability during repeated batch and perfusion cultures, using hCBiPS2 cells. **(A):** Cells were seeded at 0.5×10^6 cells per milliliter on day 0. Cell densities (columns) and viability (solid circles) were determined daily ($n = 4$). Up to 4.6-fold increase in repeated batch cultures and up to 6.7-fold increase with perfusion could be achieved. Results are reported as mean $\pm$ SEM. Differences were considered statistically significant at **, $p < .01$ and ***, $p < .001$. **(B):** Highest specific growth rates μ were observed on day 2 of cultivation (between 24 and 48 hours after inoculation). Abbreviation: d, day.

expression (Fig. 6C). In contrast, 2D precultures appeared most distant to all suspension samples, apparently reflecting 2D to 3D transition including the lack of matrix supplementation in 3D [33].

Gene ontology (GO) analysis on more than twofold regulated genes in 2D precultures versus day 7 bioreactor-derived aggregates indeed revealed that the categories "cell and biological adhesion" were among those with the highest enrichment *p* values (supplemental online Fig. 4B, 4C). These categories included the genes cell adhesion molecule 2 (*CADM2*), H-cadherin (*CDH13*), cadherin 18 (*CDH18*), protocadherin 7 (*PCDH7*), and tight junction-related claudin 11 (*CLD11*), confirming differences in cell–cell and cell–matrix adhesion in 2D versus 3D [33].

PCA further showed that day 7 repeated batch and perfusion samples appeared somewhat diverged from the tightly clustered day 3 suspension cells, whereby day 7 perfusion appeared most distant, suggesting a more pronounced impact of the feeding strategy on gene expression at later process stages (Fig. 6C).

GO analyses on more than twofold-upregulated genes in day 7 perfusion versus repeated batch aggregates showed an enrichment in categories such as "regulation of growth" (including the wingless-type MMTV integration site family [*WNT10B*], insulin-like growth factor-binding protein 7 [*IGFBP7*], cluster of differentiation 36 [*CD36*], and deiodinase iodothyronine type III [*DIO3*]) and "ionotropic glutamate receptor signaling pathway" (including glutamate ionotropic receptor NMDA type subunit 2A [*GRIN2A*], glutamate receptor 2 [*GRIA2*], glutamate receptor ionotropic AMPA 4 [*GRIA4*] implicated in regulation of proliferation in neural cells [34]) at perfusion conditions (supplemental online Fig. 5A–5C, respectively).

Moreover, *CXCL1* and *-5*, members of the CXCL family, were found to be upregulated in perfusion (supplemental online Fig. 5A), confirming CXCL5 accumulation in supernatants found by MAP (supplemental online Fig. 3A).

Gene Expression Assessment Indicates Distinct Process-Dependent Changes of hPSCs' Energy Metabolism

Distinct μ and Y(qLac/qGlc) profiles (Figs. 2B, 3C) suggested process-dependent shifts of the cells' metabolism over time, prompting us to focus on respective GO categories. Array-based heat maps revealed that changes in metabolic activity were indeed reflected in gene expression patterns (Fig. 6D).

Genes in GO categories "glycolytic processes" and "regulation of glycolytic processes" were expressed at relatively high levels in the 2D precultures. These included the two rate-limiting factors in glycolysis, that is, hexokinase (*HK1*) and phosphofructokinase (*PFKP*), as well as the enzymes aldolase (*ALDOC*) and enolase (*ENO3*; Fig. 6D), in line with the notion that glycolysis is dominating in hPSCs [35, 36]. Notably, reduced expression of these genes was readily observed in day 3 suspension samples (repeated batch and perfusion) and became more pronounced in cells derived from day 7 bioreactors, whereby some recovery of expression was observed in day 7 perfusion samples only (Fig. 6D). A reversed pattern, that is, highest expression level in day 7 bioreactor samples, was found for a panel of genes in the GO category "oxidative phosphorylation," including adenylate kinase 2 (*AK2*), and in particular for the large family of NADH dehydrogenase (ubiquinone) 1α (*NDUFA*) and 1β (*NDUFB*) subcomplex-forming factors annotated in GO category "mitochondrial electron transport" (Fig. 6D).

Together, these patterns suggest progressive transition of hPSCs' metabolism from glycolysis (in 2D monolayer) toward oxidative phosphorylation (oxphos; at later stages in 3D), which was recently correlated with induction of hPSC differentiation [37]. Since our data do not indicate any sign of differentiation in multiple assays, we have examined a panel of additional genes related to the acetyl-CoA metabolism, which was recently investigated to correlate hPSCs' differentiation status to metabolic activity [37].

We either find no culture-dependent changes in the expression of, for example, ATP citrate lyase (*ACLY*; regulating the level of cytosolic Acetyl-CoA; supplemental online Fig. 5D) or have identified the upregulation of uncoupling protein 2 (*UCP2*) and in particular of acetyl-CoA synthetase (*ACSS2*) in day 7 bioreactor samples compared with 2D preculture (Fig. 5D), whereas downregulation of these markers was found by Moussaieff et al. upon transition to hPSC differentiation [37].

Perfusion Process Efficiency Is Cell Line Independent

Applying an independent hiPSC line (hHSC_F1285T_iPS2) and the low-protein medium E8 [38, 39], the perfusion process's validity and robustness was underscored. Expansion rates were approximately sixfold, achieving an average cell density of $3.01 \pm 0.21 \times 10^6$ cells per milliliter at process endpoint (Fig. 7A, 7B). The

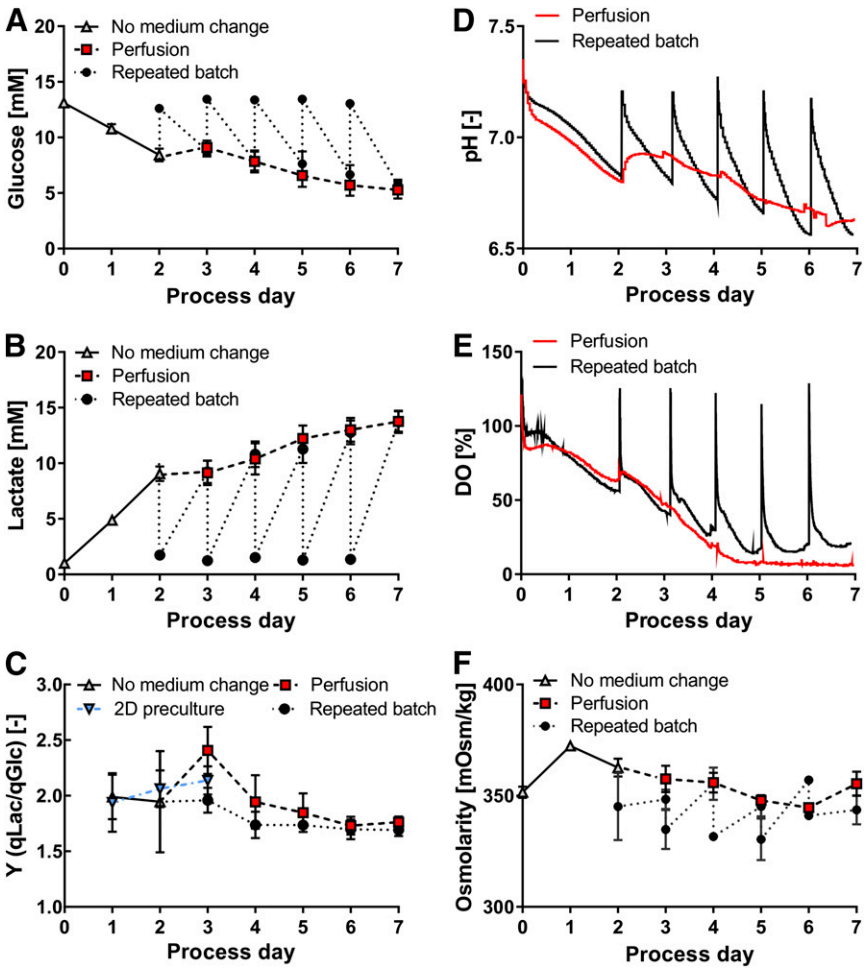

Figure 3. Metabolic activity of hCBiPS2 cells in repeated batch and perfusion cultures. Perfusion was initiated after 48 hours of culture. In parallel entire medium was replaced daily from day 2 onward in repeated batch cultures, keeping the daily and overall medium throughput equal. **(A, B):** Feeding strategies result in respective concentration pattern for glucose **(A)** and lactate **(B)** (both $n = 4$). **(C):** The specific yield coefficient of lactate from glucose Y(qLac/qGlc) is highest in the earlier process phase and decreases for both feeding strategies from process day 4 onward. **(D–F):** In response to repeated batch, heterogeneous "zigzag-like" patterns for pH **(D)** and dissolved oxygen (DO) **(E)** as well as culture osmolarity ($n = 3$) **(F)** in contrast to homogeneous progression at perfusion were observed. To ensure clarity of illustration, pH levels and dissolved oxygen are depicted for one bioreactor run of each feeding strategy. Samples for glucose, lactate, and osmolarity analysis were taken every 24 hours of culture and additionally after medium exchange for repeated batch cultures.

specific growth rate was highest during the early process phase (days 2 and 3) equivalent to hCBiPS2 cells and an even more pronounced decrease of Y(qLac/qGlc) was observed over time (from 2.0 on day 1 to 1.5 on day 7; Fig. 7D). Maintenance of pluripotency of day 7-derived cells was corroborated by flow cytometry (Fig. 7E), qRT-PCR (Fig. 7F), and microarray analysis for pluripotency-associated genes and early differentiation markers (supplemental online Fig. 6A, 6B). Notably, microarray analysis confirmed the, by trend, indicated progressive shift of hPSCs' metabolism from glycolysis in 2D precultures and at early process stages toward oxidative phosphorylation in day 7 cells (Fig. 7G), whereby largely overlapping patterns for both cell lines were observed (compare Fig. 6D with Fig. 7G). Finally, focusing on a panel of acetyl-CoA metabolism-related genes whose drastic downregulation (that is, two- to fivefold) was recently correlated with metabolic changes at early stages of differentiation [37] revealed only minor or diverse expression changes along our processes, confirmed by both cell lines tested (supplemental online Figs. 5D, 6C).

Discussion

Establishing efficient and economically viable production of hPSCs is indispensable to fuel their envisioned routine application in regenerative medicine and drug discovery [3]. The field is now reaching consensus that stirred-tank bioreactor technology is a potent approach to achieve this goal [40, 41].

Several recent studies have employed matrix-free hPSC aggregate culture in stirred vessels, applying manual medium exchange [10, 11, 15, 16, 41, 42]. Overall, applicability of the suspension culture approach for hPSC mass production was underscored and maintenance of pluripotency and karyotypic stability was confirmed.

Whereas approximately two- to fourfold expansion per passage was shown in some studies [10, 11, 15], substantially higher rates were published by others [16, 42]. However, relatively high expansion rates of up to ~12-fold per passage seem to result from low-density inoculation, e.g., at 0.2×10^5 cells per milliliter [16], finally yielding 2.4×10^5 cells per milliliter at

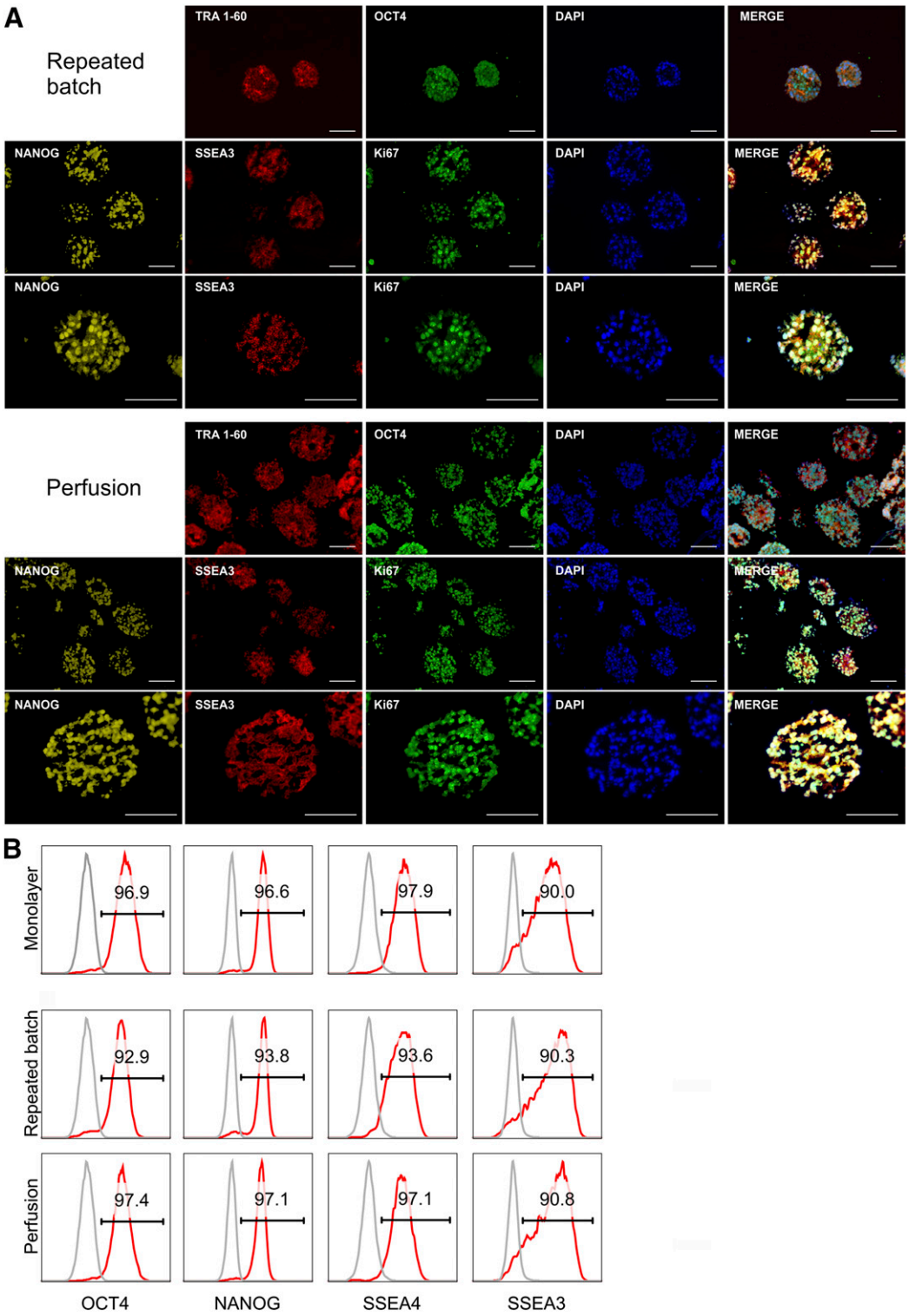

Figure 4. Pluripotency marker expression of hCBiPS2 cells after expansion with different feeding strategies. **(A):** Immunofluorescence of cryosections of aggregates harvested at process day 7 showed positive staining for the pluripotency-associated markers TRA1-60, SSEA3, OCT4, and NANOG as well as the proliferation-associated marker Ki-67. Respective isotype controls confirmed specificity of staining (data not shown). Scale bars = 100 μm. **(B):** Flow cytometry revealed that the majority of repeated batch- and perfusion-expanded cells expressed pluripotency-associated surface markers SSEA4 and SSEA3 as well as the transcription factors NANOG and OCT4 comparable to monolayer precultures (isotype control shown in gray). Abbreviation: DAPI, 4′,6-diamidino-2-phenylindole.

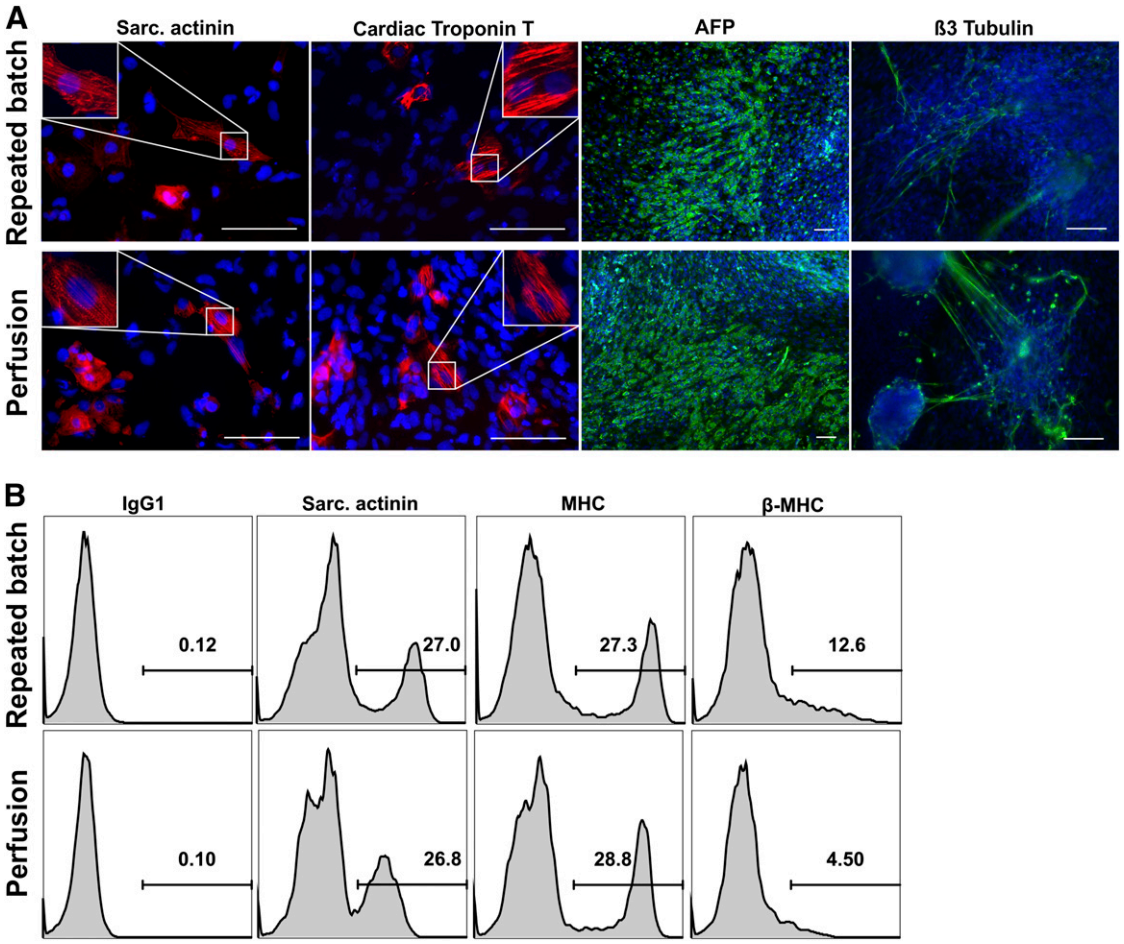

Figure 5. Repeated batch and perfusion bioreactor-expanded hCBiPS2 cells differentiate into derivatives of all three germ layers. **(A):** Immunofluorescence analysis of day 7 bioreactor-derived aggregates from repeated batch as well as perfusion cultures induced for spontaneous differentiation revealed expression of marker proteins representative of all three germ layers (positive staining in red or green): sarcomeric actinin, cardiac Troponin T (mesoderm), α-fetoprotein (AFP) (endoderm), and β3 Tubulin (ectoderm). Nuclei were stained with 4′,6-diamidino-2-phenylindole (blue). Respective isotype controls confirmed specificity of stainings (data not shown). Scale bars = 100 μm. **(B):** Furthermore, modulation of the Wnt pathway by small molecules resulted in cardiac differentiation of cells from repeated batch as well as perfusion cultures. Expression of cardiac-specific markers sarcomeric actinin and αMHC as well as βMHC could be detected by flow cytometry. Abbreviations: MHC, major histocompatibility complex; sarc., sarcomeric.

optimized conditions, which is a rather low value inapplicable for therapeutic cell production.

Here, we have applied pre-established seeding of 5×10^5 cells per milliliter, closely recapitulating former yields of $\sim 2 \times 10^6$ cells per milliliter (approximately fourfold expansion) achieved in repeated batch processes [15]. This demonstrates high process reproducibility and straightforward transition from previously used glass to single-use vessels. Importantly, using the same medium throughput established for repeated batch (i.e., 1× process volume per day), perfusion enabled us to achieve significantly higher cell line-independent cell densities of $\sim 3 \times 10^6$ cells per milliliter on average (up to 3.6×10^6 cells per milliliter in individual runs), representing approximately sixfold expansion per passage (Figs. 2A, 7A). Consequently, perfusion enabled ~43% less medium consumption compared with conventional 2D culture ("process efficiency index" calculations in supplemental online Table 1). As stirring conditions were identical at both feeding conditions and, apparently, compatible with higher cell yields and with the formation of larger aggregates in perfusion cultures (Fig. 1B–1D), it seems unlikely that the applied agitation restricts hPSC proliferation and aggregate growth, in contrast to previous concerns in an equivalent system [15]. Our calculations suggest that the 47% higher cell yield at perfusion seems mainly mediated by the concomitant increase of the aggregate volume by 33%. To our best knowledge, the achieved cell density and the overall yield of $\sim 3 \times 10^8$ cells per 100 ml in perfusion cultures is an unmet result for hPSCs grown as stirred cell-only aggregates. We acknowledge, however, that Bardy et al. have published 6.1×10^6 cells per milliliter in a microcarrier-based approach [43].

Perfusion previously enabled a culture density of $> 2 \times 10^7$ cells per milliliter for mouse PSCs [20, 21, 44]. However, in addition to species inherent differences in proliferation kinetics, this was achieved by mitogen-rich fetal calf serum-supplemented media [44] or reflects high medium throughput, e.g., by consumption of 5× process volumes per day [20, 21]. Initial studies on human ESC grown as matrix-attached monolayer [22] or microcarrier culture [12] also indicated supportive effects of perfusion, but the underlying mechanisms are not well understood.

Monitoring glucose, lactate, pH, and DO levels in our cultures, we noted that the peak values of these process

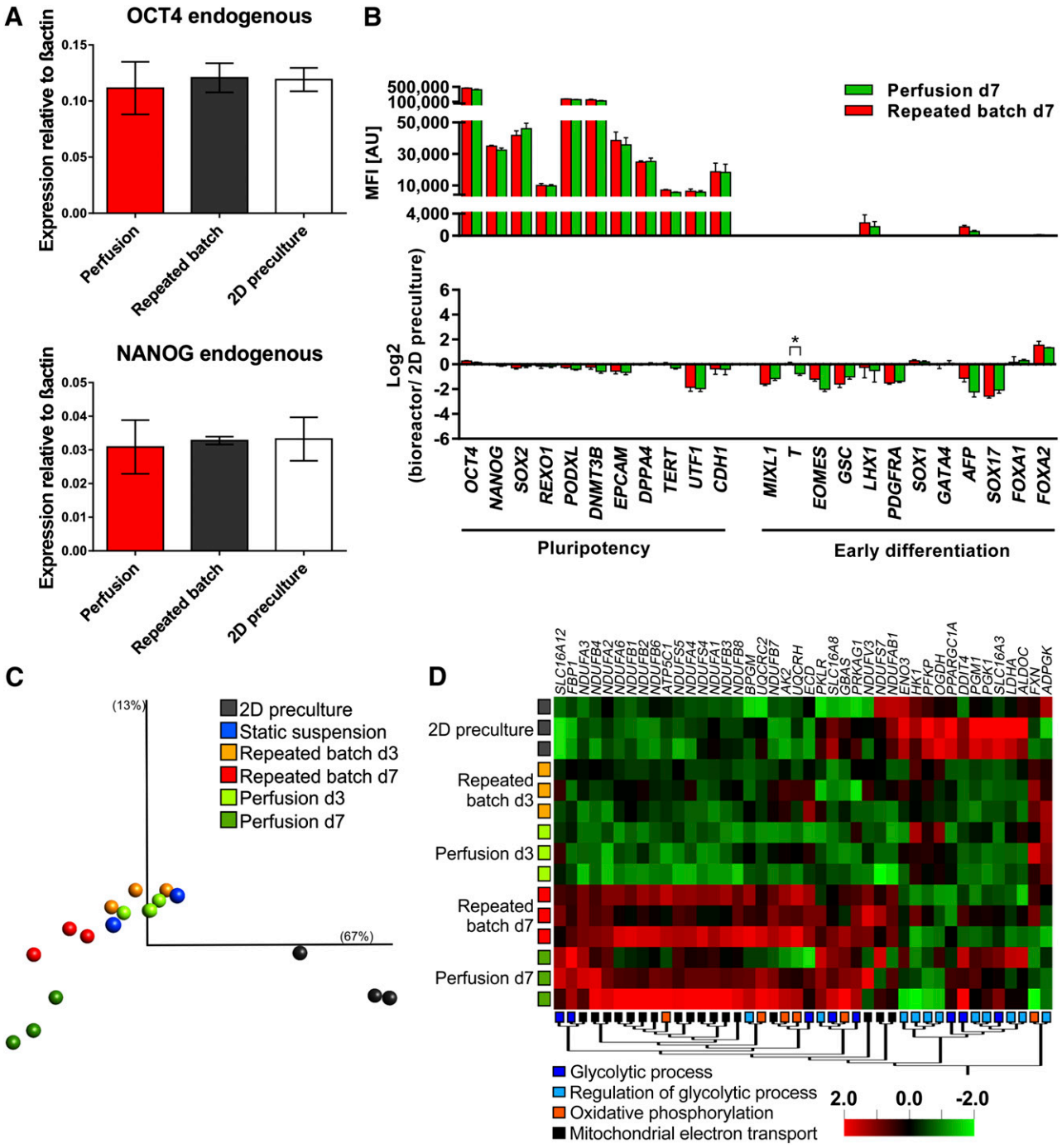

Figure 6. Expression analysis revealed high similarity between hCBiPS2 cells from 2D precultures and 3D suspension culture. **(A):** Quantitative real-time analysis for transcription factors *OCT4* and *NANOG* showed no significant deviation in expression levels of expanded cells either under repeated batch or under perfusion conditions and furthermore compared with 2D precultures ($n = 3$). Primers were defined to detect endogenous variant of the factor to exclude false positive results in induced pluripotent stem cells. **(B):** Expression levels of genes associated with pluripotency and early differentiation for repeated batch and perfusion-based cultures displayed as absolute processed fluorescence intensity (top) and compared with 2D precultures (bottom, $n = 3$). **(C):** Principle component analysis on global gene expression of hiPSC 2D precultures on day 3 (gray), static suspension cultures on day 3 (blue), dynamic suspension cultures with either perfusion or repeated batch on day 3 (perfusion, light green; repeated batch, orange), or process endpoint day 7 (perfusion, dark green; repeated batch, red). Visualization comprises >100 genes with $\sigma/\sigma\max < 0.255$ and $p < .001$ in a group comparison. See also supplemental online Figure 4A for details of the experimental setup. **(D):** The hierarchically clustered heat map displays differentially expressed genes between 2D precultures, repeated batch (day 3 and day 7), and perfusion (day 3 and day 7) samples of genes allocated to the GO categories "glycolytic process," "regulation of glycolytic process," "oxidative phosphorylation," and "mitochondrial electron transport" (multigroup comparison; $p < .1$). The microarray dataset presented in this figure was deposited in Array Express with accession no. E-MTAB-3898 (http://www.ebi.ac.uk/arrayexpress/experiments/E-MTAB-3898). Abbreviation: d, day.

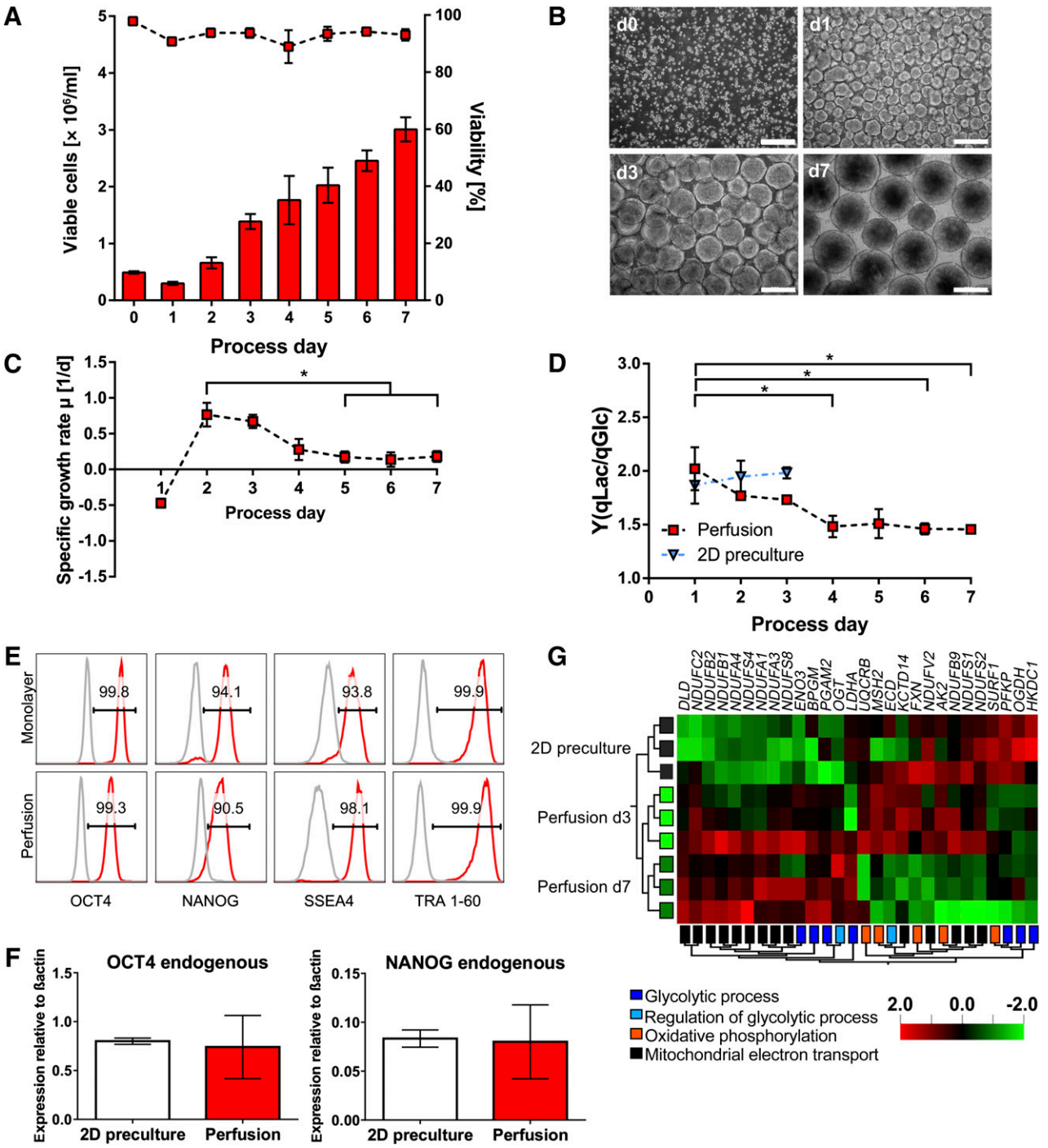

Figure 7. Characterization of perfusion cultures using hHSC_F1285T_iPS2 cells confirmed the robustness of the expansion process. **(A):** An average viable cell density of 3.01×10^6 cells per milliliter was obtained in 7-day lasting perfusion cultures representing an approximately sixfold hPSC expansion. Cell densities (columns) and viability (symbols) were determined daily ($n = 3$). **(B):** Representative microscopic images of aggregate formation and progression (scale bars = 200 μm). **(C, D):** Specific growth rate **(C)** and yield coefficient of lactate from glucose Y(qLac/qGlc) **(D)** were highest in earlier process phase for the independent second cell line as well (both $n = 3$). Results are reported as mean ± SEM. Differences were considered statistically significant at $*$, $p < .05$. **(E):** Flow cytometry analysis revealed that the majority of cells harvested on day 7 were positive for pluripotency markers OCT4, NANOG, SSEA4, and TRA 1-60 (red; isotype in gray). **(F):** Quantitative real-time analysis for pluripotency transcription factors *OCT4* and *NANOG* revealed no significant deviation in expression levels for cells harvested on day 7 compared with 2D monolayer precultures ($n = 3$). Primers were defined to detect endogenous variant of the gene only. **(G):** Hierarchically clustered heatmap displaying differentially expressed genes between 2D preculture and perfusion (day 3 and day 7) samples allocated to the GO categories "glycolytic process," "regulation of glycolytic process," "oxidative phosphorylation," and "mitochondrial electron transport" (multigroup comparison: $p < .1$). The microarray dataset presented in this figure was deposited in Array Express with accession no. E-MTAB-4149 (http://www.ebi.ac.uk/arrayexpress/experiments/E-MTAB-4149). Abbreviation: d, day.

parameters were essentially equivalent in both feeding conditions (Fig. 3). Highest lactate concentrations, for example, did not exceed 14 mM at both feeding conditions. Chen et al. showed no negative effect of 11 mM lactate on hESC growth whereas 22 mM induced substantial growth retardation [14], suggesting that lactate concentrations did not affect cell proliferation in our processes. The underlying process-dependent differences seem rather to result from smooth progression of respective parameters in perfusion in contrast to drastic oscillations in repeated batch cultures. Among other changes, repeated batch induces drastic oscillation of pH patterns and some fluctuation of medium osmolarity as well (Fig. 3D, 3F). Both pH dynamics and osmotic stress are known to act detrimentally on somatic cell viability and to trigger proliferation and metabolic changes in tumor cells [45, 46] but their impact on hPSC culture and differentiation is poorly studied [14, 47]. Notably, to ensure meaningful side-by-side comparison of the alternative feeding strategies, we focused on monitoring resulting changes of pH, DO, and other process parameters but refrained from controlling them, which, per se, is enabled by the applied bioreactor system.

However, whereas repeated batch "resets" the culture medium composition at every feed, perfusion may allow accumulation of paracrine factors (Fig. 3). Supernatant analysis revealed increased levels of CXCL5 in perfusion cultures (supplemental online Fig. 3A). CXCL5 supplementation showed some growth-promoting tendency in control experiments (supplemental online Fig. 3B), suggesting that cell-born mitogens may, to some degree, mediate the increased cell yield at perfusion. Interestingly, Krtolica et al. found that hESCs express *CXCR2*, the receptor for CXCL5 and CXCL1. However, in our suspension culture approach using hiPSCs, we could not confirm the proliferation-promoting effect of CXCL1 as described in conventional 2D hESC culture [31].

Accumulation of glutamate, alanine, and to some degree glycine was observed in our bioreactor processes in line with other studies [14, 48, 49]. Although consumed in our study, asparagine, isoleucine, histidine, and threonine have been described to be secreted by hESCs in microcarrier-based bioreactor approaches [14, 49], indicating cell line and/or process-dependent variability in hPSCs' amino acid metabolism. In CHO cells and other fast-proliferating cells, glycine production has been associated with high rates of serine metabolism whereas glutamate and alanine accumulation was reported to indicate distinct glutamine metabolism activity [50, 51]. Glutamate is known as an intermediate in the catabolism of many amino acids before ultimately converted to α-ketoglutarate, which is subsequently discharged into the tricarbon acid cycle (TCA). The reduced secretion of glutamate at days 3–7 may hint toward a change in glutamine metabolism in the second process phase (after days 3–4), especially in perfusion cultures. In the transamination pathway of the glutamine metabolism, glutamate is also reported to be converted to α-ketoglutarate while generating alanine [50, 52, 53], which might explain the accumulation of alanine observed by us. The, by trend, reduced consumption rates for several amino acids—e.g., isoleucine, leucine, methionine, phenylalanine—underscore possible changes of cells' metabolism over time as indicated by our gene expression results.

Research on somatic cell reprogramming recently stimulated investigations on PSCs' metabolism along the transition to pluripotency [54]. Oxphos, the typical energy metabolism in somatic cells in the presence of oxygen, is specified by directing glucose-derived pyruvate (catalyzed to acetyl-CoA) to the tricarbon acid cycle in mitochondria, where stepwise electron transfer to oxygen is catalyzed, resulting in efficient ATP synthesis and the production of CO_2. In contrast, PSCs, which have immature mitochondria, mainly rely on glycolysis for ATP synthesis even if ample oxygen is available at atmospheric conditions [55]. This phenomenon is known as "anaerobic respiration" or the Warburg effect and is well established for highly proliferative tumor cells [56] and at early stages of embryogenesis [36].

Although the impact of oxygen concentration on hPSC proliferation and pluripotency remains controversially discussed [55], recent work substantiated that PSCs rely on glycolysis to generate the required metabolic building blocks to fuel the synthesis of DNA, protein, and the membrane component, whose availability is a bottleneck in fast-proliferating cells [57]. Moussaieff et al. further highlighted that glycolysis fuels high cytosolic Acetyl-CoA levels necessary to ensure chromatin acetylation in PSCs, thereby stabilizing the pluripotent state [37].

Our study reveals intriguing results when aligning growth kinetics, metabolic changes, and gene expression patterns. The highest specific growth rate μ of 0.81 day^{-1}, known for hPSCs at optimal proliferation conditions [25, 58], was observed at day 2; at this early stage Y(qLac/qGlc) was $\sim$2.0 for bioreactor cultures, equivalent to values observed in the 2D precultures (Figs. 3C, 7D), which is typical for glycolysis. Already between process days 2 and 3 a relatively drastic drop of μ was observed with μ finally ranging from $\sim$0.2 to 0.3 day^{-1} on days 4–7 for both independent cell lines (Figs. 2B, 7C). Despite some perfusion-induced delay, these data indicate a proliferation-confining environment readily at early process stages although no obvious nutrition limits were suggested, at least by the glucose and amino acid concentrations as well as aggregate sizes; diffusion limits are thought to occur at $>$300 μm diameter [59].

However, Y(qLac/qGlc) maintained at higher levels at perfusion until day 5 but ultimately decreased to $\sim$1.6 at both process strategies (Fig. 3C). Notably, this value is typical of oxphos in differentiated, somatic cells where Y(qLac/qGlc) ranges from 1.5 to 1.7 [60]. Considering the concomitant changes in the expression pattern of key metabolic marker genes, our data suggest that hPSCs have indeed shifted their energy metabolism from glycolysis more toward oxphos along our bioreactor processes, but notably in the absence of differentiation, as fully confirmed by an independent cell line (Figs. 4–7). Our findings are unexpected in the light of a recent study showing that the metabolic switch from glycolysis to oxphos is closely coupled to hPS cell differentiation [37]; thus our data reveal a surprising level of "metabolic plasticity" in hPSCs. This further suggests that the (yet suboptimal) environment in suspension culture (which is likely mediated by numerous cues including paracrine factors, pH and DO drops, and/or others) acts restrictively on hPSC proliferation and triggers the metabolic shift toward oxphos. Recent studies utilizing stirred-tank bioreactors showed that controlling oxygen at higher levels improved hPSC expansion compared with lower, supposedly hypoxic levels [11, 12]. Although the transient restoration of high DO levels in the repeated-batch processes in our study had no apparent positive effect on hPSC growth, we cannot exclude that the overall drop in DO throughout both processes affects the cell's energy metabolism and growth kinetics and cell yield [61]. Thus, controlling this parameter will be crucial in future studies, which can be more rigorously achieved in perfused processes.

"Protective mechanisms" apparently avoid hPSC differentiation in the later process phase. These mechanisms likely

include the presence of bFGF and transforming growth factor β in the culture medium, maintaining not only the expression of typical pluripotency markers but eventually also that of metabolic enzymes such as ACLY and ACSS, which, according to Moussaieff et al. [37], stabilize hPSCs' pluripotency by catalyzing high cytosolic acetyl-CoA levels and thus chromatin acetylation.

Applying repeated batch feeding of hESCs on matrix-coated microcarriers in a stirred bioreactor, Silva et al. recently found elevated glycolysis in 3D suspension culture compared with 2D static controls [49]. Since the same culture medium (mTeSR1) was used, the study seemingly contradicted our results. However, key differences include the maintained presence of a matrix and an entirely different growth kinetic in the microcarrier approach, i.e., a 4- to 5-day lag phase postinoculation followed by exponential growth on days ~6–10. The opposition of both studies underscores the culture environment-dependent plasticity of hPSCs and highlights the value of metabolic and global transcriptome analysis for process development.

Conclusion

To the best of our knowledge this study is the first to describe the expansion of hPSCs in fully instrumented single-use stirred-tank bioreactors and an in-depth parallel investigation of alternative feeding strategies. By automated continuous perfusion a more efficient and homogenous hPSC expansion process yielding a superior cell density of up to 3.6×10^6 cells per milliliter was established. According to Wang et al. [41], processing at higher cell density is advantageous for large-scale production due to the higher conversion efficiency of labor and media.

Further steps toward the mass cultivation of hPSCs include exceeding the current culture scale toward 1.000 ml and beyond as well as the control of key process parameters. Since repeated batch cultures cannot provide homogeneous operating conditions fundamental for the control of DO and pH, the establishment of an automated perfusion mode represents a substantial step toward the controlled mass expansion of hPSCs.

Acknowledgments

We thank the Research Core Unit (RCU) Transcriptomics at Hannover Medical School for performing microarray experiments, Dr. A. Haase for providing hiPSCs, and Martina Weiss at Leibniz University Hannover for providing technical assistance. This work was funded by the German Research Foundation (DFG) (including the projects Cluster of Excellence REBIRTH DFG EXC62/3, ZW 64/4-1, and MA2331/16-1), the German Ministry for Education and Science (BMBF) (Grant 13N12606), StemBANCC (support from the Innovative Medicines Initiative joint undertaking under Grant 115439-2, whose resources are composed of financial contribution from the European Union [FP7/2007-2013] and EFPIA companies' in-kind contribution), and TECHNOBEAT (European Union H2020, GA no. 668724).

Author Contributions

C.K. and H.K.: collection and assembly of data, data analysis and interpretation, article writing; C.H., D.R.-D., and A.F.: collection of data; T.S., T.K., and T.O.J.: provision of analytical technologies, collection of data; K.K.: provision of study material; A.H. and U.M.: conception and design, financial support; R.Z.: conception and design, data analysis and interpretation, article writing, financial support; R.O.: conception and design, collection and assembly of data, data analysis and interpretation, article writing.

Disclosure of Potential Conflicts of Interest

K.K. has compensated employment. T.O.J. is a compensated scientific advisor for Myriad RBM and has contracted research paid to Natural and Medical Sciences Institute (NMI): Bayer, Abbvie, Roche, HOT Screen GmbH. The other authors indicated no potential conflicts of interest.

References

1 Inoue H, Nagata N, Kurokawa H et al. iPS cells: A game changer for future medicine. EMBO J 2014;33:409–417.

2 Kempf H, Andree B, Zweigerdt R. Large-scale production of human pluripotent stem cell derived cardiomyocytes. Adv Drug Deliv Rev 2016;96:18–30.

3 Zweigerdt R. Large scale production of stem cells and their derivatives. Adv Biochem Eng Biotechnol 2009;114:201–235.

4 Serra M, Brito C, Correia C et al. Process engineering of human pluripotent stem cells for clinical application. Trends Biotechnol 2012;30: 350–359.

5 Bareither R, Pollard D. A review of advanced small-scale parallel bioreactor technology for accelerated process development: Current state and future need. Biotechnol Prog 2011;27: 2–14.

6 Olmer R, Haase A, Merkert S et al. Long term expansion of undifferentiated human iPS and ES cells in suspension culture using a defined medium. Stem Cell Res (Amst) 2010; 5:51–64.

7 Singh H, Mok P, Balakrishnan T et al. Up-scaling single cell-inoculated suspension culture of human embryonic stem cells. Stem Cell Res (Amst) 2010;4:165–179.

8 Zweigerdt R, Olmer R, Singh H et al. Scalable expansion of human pluripotent stem cells in suspension culture. Nat Protoc 2011;6: 689–700.

9 Amit M, Chebath J, Margulets V et al. Suspension culture of undifferentiated human embryonic and induced pluripotent stem cells. Stem Cell Rev 2010;6:248–259.

10 Chen VC, Couture SM, Ye J et al. Scalable GMP compliant suspension culture system for human ES cells. Stem Cell Res (Amst) 2012;8: 388–402.

11 Abbasalizadeh S, Larijani MR, Samadian A et al. Bioprocess development for mass production of size-controlled human pluripotent stem cell aggregates in stirred suspension bioreactor. Tissue Eng Part C Methods 2012;18:831–851.

12 Serra M, Brito C, Sousa MF et al. Improving expansion of pluripotent human embryonic stem cells in perfused bioreactors through oxygen control. J Biotechnol 2010;148:208–215.

13 Ting S, Chen A, Reuveny S et al. An intermittent rocking platform for integrated expansion and differentiation of human pluripotent stem cells to cardiomyocytes in suspended microcarrier cultures. Stem Cell Res (Amst) 2014;13: 202–213.

14 Chen X, Chen A, Woo TL et al. Investigations into the metabolism of two-dimensional colony and suspended microcarrier cultures of human embryonic stem cells in serum-free media. Stem Cells Dev 2010;19:1781–1792.

15 Olmer R, Lange A, Selzer S et al. Suspension culture of human pluripotent stem cells in controlled, stirred bioreactors. Tissue Eng Part C Methods 2012;18:772–784.

16 Hunt MM, Meng G, Rancourt DE et al. Factorial experimental design for the culture of human embryonic stem cells as aggregates in stirred suspension bioreactors reveals the potential for interaction effects between bioprocess parameters. Tissue Eng Part C Methods 2014;20:76–89.

17 Castilho L, Medronho R. Cell retention devices for suspended-cell perfusion cultures.

In: Scheper T, ed. Advances in Biochemical Engineering/ Biotechnology. 1st ed. New York: Springer Berlin Heidelberg, 2002:129–169.

18 Chu L, Robinson DK. Industrial choices for protein production by large-scale cell culture. Curr Opin Biotechnol 2001;12:180–187.

19 Tao Y, Shih J, Sinacore M et al. Development and implementation of a perfusion-based high cell density cell banking process. Biotechnol Prog 2011;27:824–829.

20 Fernandes-Platzgummer A, Diogo MM, da Silva CL et al. Maximizing mouse embryonic stem cell production in a stirred tank reactor by controlling dissolved oxygen concentration and continuous perfusion operation. Biochem Eng J 2014;82:81–90.

21 Baptista RP, Fluri DA, Zandstra PW. High density continuous production of murine pluripotent cells in an acoustic perfused bioreactor at different oxygen concentrations. Biotechnol Bioeng 2013;110:648–655.

22 Fong WJ, Tan HL, Choo A et al. Perfusion cultures of human embryonic stem cells. Bioprocess Biosyst Eng 2005;27:381–387.

23 Kempf H, Kropp C, Olmer R et al. Cardiac differentiation of human pluripotent stem cells in scalable suspension culture. Nat Protoc 2015; 10:1345–1361.

24 Weegman BP, Nash P, Carlson AL et al. Nutrient regulation by continuous feeding removes limitations on cell yield in the large-scale expansion of mammalian cell spheroids. PLoS One 2013;8:e76611.

25 Haase A, Olmer R, Schwanke K et al. Generation of induced pluripotent stem cells from human cord blood. Cell Stem Cell 2009; 5:434–441.

26 Hartung S, Schwanke K, Haase A et al. Directing cardiomyogenic differentiation of human pluripotent stem cells by plasmid-based transient overexpression of cardiac transcription factors. Stem Cells Dev 2013;22: 1112–1125.

27 Paleček J, Zweigerdt R, Olmer R et al. A practical synthesis of Rho-Kinase inhibitor Y-27632 and fluoro derivatives and their evaluation in human pluripotent stem cells. Org Biomol Chem 2011;9:5503–5510.

28 Fernandes TG, Fernandes-Platzgummer AM, da Silva CL et al. Kinetic and metabolic analysis of mouse embryonic stem cell expansion under serum-free conditions. Biotechnol Lett 2010;32:171–179.

29 Varum S, Rodrigues AS, Moura MB et al. Energy metabolism in human pluripotent stem cells and their differentiated counterparts. PLoS One 2011;6:e20914.

30 Glacken MW. Catabolic control of mammalian-cell culture. Biotechnology (N Y) 1988;6:1041.

31 Krtolica A, Larocque N, Genbacev O et al. GROα regulates human embryonic stem cell self-renewal or adoption of a neuronal fate. Differentiation 2011;81:222–232.

32 Kempf H, Olmer R, Kropp C et al. Controlling expansion and cardiomyogenic differentiation of human pluripotent stem cells in scalable suspension culture. Stem Cell Rep 2014;3:1132–1146.

33 Konze SA, van Diepen L, Schröder A et al. Cleavage of E-cadherin and β-catenin by calpain affects Wnt signaling and spheroid formation in suspension cultures of human pluripotent stem cells. Mol Cell Proteomics 2014;13: 990–1007.

34 Willard SS, Koochekpour S. Glutamate signaling in benign and malignant disorders: Current status, future perspectives, and therapeutic implications. Int J Biol Sci 2013;9: 728–742.

35 Dong C, Yuan T, Wu Y et al. Loss of FBP1 by Snail-mediated repression provides metabolic advantages in basal-like breast cancer. Cancer Cell 2013;23:316–331.

36 Shyh-Chang N, Daley GQ, Cantley LC. Stem cell metabolism in tissue development and aging. Development 2013;140:2535–2547.

37 Moussaieff A, Rouleau M, Kitsberg D et al. Glycolysis-mediated changes in acetyl-CoA and histone acetylation control the early differentiation of embryonic stem cells. Cell Metab 2015;21:392–402.

38 Chen G, Gulbranson DR, Hou Z et al. Chemically defined conditions for human iPSC derivation and culture. Nat Methods 2011;8: 424–429.

39 Wang Y, Chou BK, Dowey S et al. Scalable expansion of human induced pluripotent stem cells in the defined xeno-free E8 medium under adherent and suspension culture conditions. Stem Cell Res (Amst) 2013;11:1103–1116.

40 Sart S, Schneider YJ, Li Y et al. Stem cell bioprocess engineering towards cGMP production and clinical applications. Cytotechnology 2014;66:709–722.

41 Wang Y, Cheng L, Gerecht S. Efficient and scalable expansion of human pluripotent stem cells under clinically compliant settings: A view in 2013. Ann Biomed Eng 2014;42: 1357–1372.

42 Krawetz R, Taiani JT, Liu S et al. Large-scale expansion of pluripotent human embryonic stem cells in stirred-suspension bioreactors. Tissue Eng Part C Methods 2010;16:573–582.

43 Bardy J, Chen AK, Lim YM et al. Microcarrier suspension cultures for high-density expansion and differentiation of human pluripotent stem cells to neural progenitor cells. Tissue Eng Part C Methods 2013;19:166–180.

44 Niebruegge S, Nehring A, Bär H et al. Cardiomyocyte production in mass suspension culture: Embryonic stem cells as a source for great amounts of functional cardiomyocytes. Tissue Eng Part A 2008;14:1591–1601.

45 Cardone RA, Casavola V, Reshkin SJ. The role of disturbed pH dynamics and the Na+/H+ exchanger in metastasis. Nat Rev Cancer 2005; 5:786–795.

46 Madonna R, Görbe A, Ferdinandy P et al. Glucose metabolism, hyperosmotic stress, and reprogramming of somatic cells. Mol Biotechnol 2013;55:169–178.

47 Teo AL, Mantalaris A, Lim M. Influence of culture pH on proliferation and cardiac differentiation of murine embryonic stem cells. Biochem Eng J 2014;90:8–15.

48 Christensen DR, Calder PC, Houghton FD. Effect of oxygen tension on the amino acid utilisation of human embryonic stem cells. Cell Physiol Biochem 2014;33:237–246.

49 Silva MM, Rodrigues AF, Correia C et al. Robust expansion of human pluripotent stem cells: Integration of bioprocess design with transcriptomic and metabolomic characterization. STEM CELLS TRANSLATIONAL MEDICINE 2015;4: 731–742.

50 Godia F, Cairo JJ. Cell metabolism. In: Ozturk SS, ed. Cell Culture Technology for Pharmaceutical and Cell-Based Therapies. Boca Raton: CRC Press, 2005:81–106.

51 Snell K, Natsumeda Y, Weber G. The modulation of serine metabolism in hepatoma 3924A during different phases of cellular proliferation in culture. Biochem J 1987;245: 609–612.

52 Altamirano C, Paredes C, Cairó JJ et al. Improvement of CHO cell culture medium formulation: Simultaneous substitution of glucose and glutamine. Biotechnol Prog 2000;16:69–75.

53 Hayter PM, Curling EM, Baines AJ et al. Chinese hamster ovary cell growth and interferon production kinetics in stirred batch culture. Appl Microbiol Biotechnol 1991;34: 559–564.

54 Folmes CD, Nelson TJ, Martinez-Fernandez A et al. Somatic oxidative bioenergetics transitions into pluripotency-dependent glycolysis to facilitate nuclear reprogramming. Cell Metab 2011; 14:264–271.

55 Turner J, Quek LE, Titmarsh D et al. Metabolic profiling and flux analysis of MEL-2 human embryonic stem cells during exponential growth at physiological and atmospheric oxygen concentrations. PLoS One 2014;9:e112757.

56 Levine AJ, Puzio-Kuter AM. The control of the metabolic switch in cancers by oncogenes and tumor suppressor genes. Science 2010; 330:1340–1344.

57 Vander Heiden MG, Cantley LC, Thompson CB. Understanding the Warburg effect: The metabolic requirements of cell proliferation. Science 2009;324:1029–1033.

58 Adewumi O, Aflatoonian B, Ahrlund-Richter L et al. Characterization of human embryonic stem cell lines by the International Stem Cell Initiative. Nat Biotechnol 2007;25:803–816.

59 Kinney MA, Sargent CY, McDevitt TC. The multiparametric effects of hydrodynamic environments on stem cell culture. Tissue Eng Part B Rev 2011;17:249–262.

60 Zeng AP, Hu WS, Deckwer WD. Variation of stoichiometric ratios and their correlation for monitoring and control of animal cell cultures. Biotechnol Prog 1998;14:434–441.

61 Zhang J, Nuebel E, Daley GQ et al. Metabolic regulation in pluripotent stem cells during reprogramming and self-renewal. Cell Stem Cell 2012;11:589–595.

See www.StemCellsTM.com for supporting information available online.

